

RESEARCH

Open Access



# Cell-free fat extract restores hair loss: a novel therapeutic strategy for androgenetic alopecia

Yizuo Cai<sup>1†</sup>, Zhuoxuan Jia<sup>1†</sup>, Yichen Zhang<sup>2</sup>, Bijun Kang<sup>1</sup>, Chingyu Chen<sup>1</sup>, Wei Liu<sup>1\*</sup>, Wei Li<sup>1\*</sup>  and Wenjie Zhang<sup>1\*</sup>

## Abstract

**Background** Androgenetic alopecia (AGA) is one of the most common hair loss diseases worldwide. However, current treatments including medicine, surgery, and stem cells are limited for various reasons. Cell-free fat extract (CEFFE), contains various cell factors, may have potential abilities in treating AGA. This study aims to evaluate the safety, effectiveness and the underlying mechanism of CEFFE in treating AGA.

**Methods** Sex hormone evaluation, immunogenicity assay and genotoxicity assay were conducted for CEFFE. In vivo study, male C57BL/6 mice were injected subcutaneously with dihydrotestosterone (DHT) and were treated with different concentration of CEFFE for 18 days (five groups and  $n = 12$  in each group: Control, Model, CEFFE<sup>Low</sup>, CEFFE<sup>Middle</sup>, CEFFE<sup>High</sup>). Anagen entry rate and hair coverage percentage were analyzed through continuously taken gross photographs. The angiogenesis and proliferation of hair follicle cells were evaluated by hematoxylin–eosin, anti-CD31, and anti-Ki67 staining. In vitro study, dermal papilla cells (DPCs) were incubated with different concentrations of CEFFE, DHT, or CEFFE + DHT, followed by CCK-8 assay and flow cytometry to evaluate cell proliferation cycle and apoptosis. The intracellular DHT level were assessed by enzyme-linked immunosorbent assay. The expression of 5 $\alpha$ -reductase type II, 3 $\alpha$ -hydroxysteroid dehydrogenase and androgen receptor were assessed through reverse transcription-quantitative polymerase chain reaction (RT-qPCR) or/and western blot.

**Results** In CEFFE-treated mice, an increase in the anagen entry rate and hair coverage percentage was observed. The number of CD31-positive capillaries and Ki67-positive cells were increased, suggesting that CEFFE promoted the proliferation of DPCs, modulated the cell cycle arrest, inhibited apoptosis caused by DHT, reduced the intracellular concentration of DHT in DPCs, and downregulated the expression of AR.

**Conclusions** CEFFE is a novel and effective treatment option for AGA through producing an increased hair follicle density and hair growth rate. The proposed mechanisms are through the DHT/AR pathway regulation and regional angiogenesis ability.

**Keywords** Androgenetic alopecia, Fat extract, Cell-free therapy

<sup>†</sup>Yizuo Cai and Zhuoxuan Jia are co-authors.

\*Correspondence:

Wei Liu

liuwei\_md@126.com

Wei Li

liweiboshi@163.com

Wenjie Zhang

wenjieboshi@aliyun.com

Full list of author information is available at the end of the article



## Background

Androgenetic alopecia (AGA) is a common multifactorial dermatologic condition characterized by progressive hair loss across frontotemporal and vertex scalp regions [1, 2]. The highest prevalence was found in Caucasians, and the morbidity rate gradually increases with aging [3, 4]. Although the specific mechanisms underlying AGA remains incompletely understood, the excess testosterone metabolite dihydrotestosterone (DHT) derivate from testosterone and high expression of androgen receptors (AR) are vital mediators in AGA development [5–7]. DHT binds to AR in dermal papilla cells (DPCs) regulating downstream target gene transcription, resulting in hair follicle degeneration [1, 6]. Specifically, the rapid growth phase (anagen) was shortened, and the no-growth phase (telogen) was prolonged. Over time, the terminal hair was converted into thinner and shorter villus hair [8]. Thus, altering the DHT or AR expression in DPCs is critical in androgen induced balding. Angiogenesis might also play a part in AGA, which the scalp's vascularity may be an essential environmental factor in the health of hair roots.

Currently in the market, orally taken Finasteride, and topically applied Minoxidil are used as the standard first-line treatments for AGA [9]. Finasteride, a selective steroidal inhibitor of 5- $\alpha$ -reductase could inhibit the conversion from testosterone to DHT, resulting in a decrease in serum and scalp DHT levels [10]. However, long-term usage of Finasteride is associated with rare complications like decreased libido, gynecomastia and psychologic impairments [11]. Minoxidil, on the other hand, induce vasodilation of peripheral vessels and improve microcirculation, leading to DPCs proliferation [12]. Nevertheless, topically applied Minoxidil is also absorbed into the systemic circulation and caused cardiovascular side effects [13]. Alternatively, hair follicle transplantation another way to treat AGA but is limited by the shortage of donor hair follicles, and the cost of treatment [14]. Therefore, more effective and economical approaches with fewer side effects are in urgent need to prevent AGA progression and stimulate hair regrowth.

Other than drug treatments, multipotent stem cells, such as adipose-derived stem cells (ADSCs), have been employed as attractive options for AGA therapy [15–17]. According to previous studies, stem cells mainly exert their therapeutic effects through a paracrine manner rather than differentiation into specific cell types [18, 19]. Those secreted factors, including hepatocyte growth factor (HGF), vascular endothelial growth factor (VEGF), and insulin-like growth factor (IGF), could promote angiogenesis, maintaining hair in anagen phase, and therefore activating hair growth [20–23]. However, the clinical

application of such stem cell therapy is still limited by manufacturing issues and ethical concerns.

We propose using a novel economical therapeutic agent, cell-free fat extract (CEFFE), to treat AGA. CEFFE is the liquid fraction isolated that mechanically from liposuction wastes. According to previous studies, the composition of CEFFE is similar to stem cell paracrine factors, including VEGF, IGF, and HGF, which these factors promote neovascularization and have anti-inflammatory effects [24–28]. In addition, previous study has demonstrated CEFFE as a promising therapeutic strategy for treating inflammatory disease and ischemia disorders in the limb ischemia model, tissue expansion model, and diabetic wound healing model [28, 29]. The abundant sources, ease of acquisition, and low immunogenicity of CEFFE makes clinical application possible. Thus, we proposed that CEFFE has positive effects on regulating DHT/AR signaling and modifying the angiogenesis microenvironment of AGA patients. Both in vitro and in vivo experiment has been carried out, using DHT-induced AGA models, to evaluate the protective effects of CEFFE and investigate its underlying mechanism.

## Methods

### CEFFE preparation

The study was approved by The Ethics Committee of Shanghai Ninth People's Hospital, Shanghai Jiaotong University School of Medicine, Shanghai, China (SH9H-2018-T22-1). After obtaining consent forms, adipose tissue was harvested from the abdomen or thigh of healthy adult females using liposuction from December 2020 to November 2021. In this study, CEFFE was derived from 5 females aged from 22 to 35. The preparation procedure of CEFFE followed previously established protocol [24]. Briefly, the harvested adipose tissue was flushed with physiological saline and centrifuged at 1200  $g/4$  °C for 3 min 2 or 3 times to remove tissue debris, blood, and oil. Then, the emulsified fat was obtained by mechanical emulsification through two 10 mL syringes (KDL, China) connected by a three-way stopcock with an internal diameter of 2 mm (Terumo Corporation, Japan) 60 times. Immediately after, the emulsified fat was centrifuged at 1200  $g/4$  °C for 5 min, and the liquid in the bottom was withdrawn. Finally, the extract supernatant was filtrated with a 0.22  $\mu$ m filter (Corning, USA) as CEFFE and subsequently frozen at  $-80$  °C for future experiments [24]. The protein concentration in CEFFE was determined with a bicinchoninic acid assay kit (BCA, Thermo Fisher Scientific, USA).

### Safety evaluation of CEFFE

Considering that hormones (especially testosterone) may have an effect on AGA treatment, we collected CEFFE

from 8 male patients, in which testosterone and estradiol were measured. Basic patient information was shown in Additional file 1: Table S1. For the immunogenicity and genotoxicity of CEFFE, we have done a series of tests based on ISO/IEC 17025. (1) In vitro cytotoxicity test. L929 cells were cultivated in blank control (10% FBS in  $\alpha$ -MEM medium, Gibco, UAS), negative control (complete medium containing 10% polyethylene), positive control (complete medium containing 10% DMSO, Sigma, USA), experimental groups (complete medium containing 12.5%, 25%, 50%, 100% CEFFE, respectively) 24 h and cell viability were determined by MTT assay. Cell viability less than 70% was considered potentially cytotoxic. (2) Intracutaneous reactivity test. Three healthy adult male New Zealand White rabbits (China Institute of Food and Drug Verification, China) weighing  $>2$  kg were used for the test. 0.2 mL of CEFFE was intradermally injected at five points on one side of each rabbit's spine and 0.2 mL (0.9% NaCl; blank control) was intradermally injected in the same operation on the opposite side, with 1 cm between the injection points. 24, 48, 72 h after injection, erythema and edema at the injection sites were recorded. Each rabbit was euthanized with an intravenous injection of sodium pentobarbital (100 mg/kg, China Institute of Food and Drug Verification, China) after recording. The scoring method and reference standard can be referred to [25]. If the final score was  $\leq 1$ , the sample was considered negative. (3) Systemic toxicity assay. A single dose of 50 mL/kg CEFFE was injected intraperitoneal in male Kunming mice (The weight at the time of injection was 17–23 g, and the difference between groups did not exceed  $\pm 20\%$  of the mean. China Institute of Food and Drug Verification, China) in the experimental group ( $n=5$ ), while 0.9% NaCl was applied in the control group ( $n=5$ ) according to the random number table. The animals were observed immediately following injection, 24, 48, and 72 h after application to evaluate the presence of toxic signs (weight loss, and/or death). All mice were euthanized with carbon dioxide inhalation, and the bilateral thoracotomy was used as second method to confirm the death. (4) The pyrogen test. 10 mL/kg CEFFE was injected to three healthy young adult male New Zealand White rabbits (China Institute of Food and Drug Verification, China) weighing  $>1.7$  kg. The baseline rectal temperature was recorded every 30 min for one hour before the injection. After one hour, rabbits were inoculated in the ear

marginal vein. Temperatures were recorded every 30 min for three hours after the injection. Each rabbit was euthanized with an intravenous injection of sodium pentobarbital (100 mg/kg, China Institute of Food and Drug Verification, China) after recording. The test indicates the presence of a pyrogen when one of the three rabbits shows an increase in body temperature higher than  $0.6$  °C or when the sum of the maximum temperature rises in the three individual rabbits exceeds  $1.3$  °C. (5) Bacterial assay for gene Mutation-Ames test. Salmonella typhimurium histidine-requiring strains TA97, TA98, TA100, and TA102 were exposed to negative control, positive control and CEFFE respectively, the specific system was shown in Additional file 1: Table S5. The number of colonies in the positive control group should be more than 3 times that of the negative control group. If the number of colonies in the experimental group increases more than twice compared with the negative control group, it is a positive reaction. (6) Mouse lymphoma TK assay (MLA assay). Specific steps could be referred to [26], and the specific system was shown in Additional file 1: Table S6.

#### Animals and experimental design

All animal experiments were approved by the Ethics Committee of Shanghai Jiao Tong University (SH9H-2021-A183-SB) carried out according to ARRIVE guidelines (<https://www.nc3rs.org.uk/arrive-guidelines>). Sixty male C57BL/6 mice (5–6 weeks old,  $23.02 \pm 2.0$  g) were purchased from Charles River (Charles River Laboratories, China) and raised under standard conditions with constant temperature and humidity under 12-h phase light–dark cycle. Drinking water and food were freely available. During the experiment, all mice were kept on the same cage shelf in an animal room.

Group-specific methods and treatments were presented in Fig. 1A, B and summarized below. The sample size was calculated based on our pre-experimental results. Mice were divided into five groups randomly ( $n=12$  in each group) according to the random number table: Control, Model, CEFFE<sup>Low</sup>, CEFFE<sup>Middle</sup>, and CEFFE<sup>High</sup>. The experiment was divided into two consecutive phases: a modeling phase (D-14 to D-1) and a treatment phase (D0 to D16). During the modeling phase, subjects in all other groups except the control group were injected subcutaneously at the nape of the neck with DHT (2 mg/kg) every day [30, 31]. To synchronize the hair cycle [32, 33], both sides of all mice's dorsal

(See figure on next page.)

**Fig. 1** Therapeutic efficacy of cell-free fat extract (CEFFE) in dihydrotestosterone (DHT)-induced androgenic alopecia (AGA) C57BL/6 mouse models. **A** Schematic diagram of experimental design for CEFFE treatment in DHT-induced AGA C57BL/6 mouse models. **B** Flowchart of the dosing regimen and behavioral experiments. **C** Representative dorsal skin images of different groups from D0 to D16. **D** Anagen entry ratio (%) and corresponding timeline from D0 to D16. **E** Hair growth ratio (%) on the dorsal skin for each group from D6 to D16. Statistical Data represent the mean  $\pm$  SD;  $n=12$ ;  $*P<0.05$

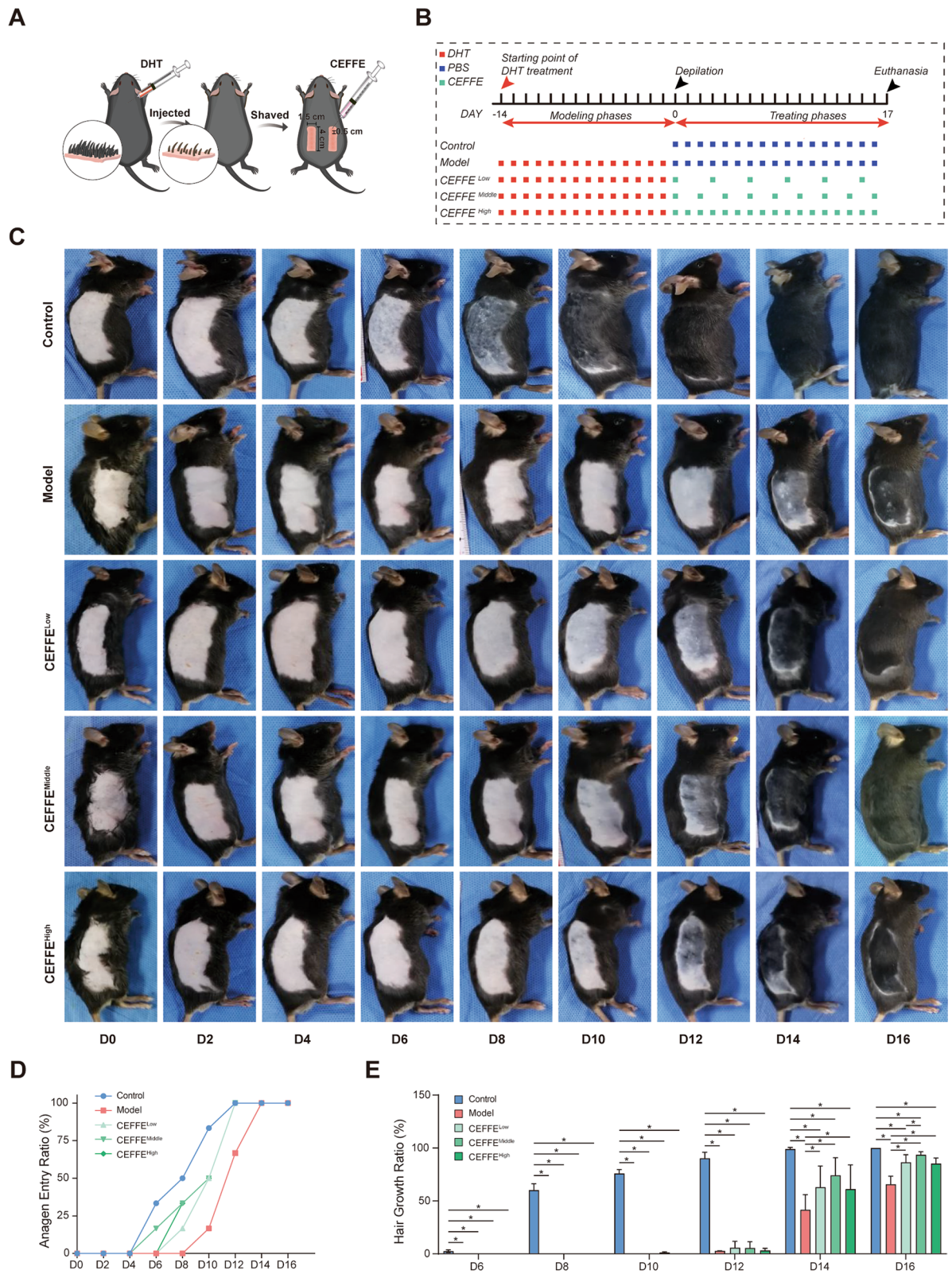


**Fig. 1** (See legend on previous page.)

areas ( $4 \times 1.5 \text{ cm}^2$ ) were shaved using an electric clipper followed by depilatory cream to remove residual hair on D0. Entering the treatment phase, all subjects in the Control and Model group were injected subcutaneously with 100  $\mu\text{L}$  PBS per day into the shaved areas. Mice in the CEFFE<sup>Low</sup>, CEFFE<sup>Middle</sup>, and CEFFE<sup>High</sup> groups were treated with 100  $\mu\text{L}$  CEFFE (3  $\mu\text{g}/\mu\text{L}$ ) at 3 days, 2 days, and 1 day interval respectively. All mice were euthanized with carbon dioxide inhalation, and the bilateral thoracotomy was used as second method to confirm the death on the 17th day, and the center region of previously shaved dorsal skin was acquired for further histology analysis.

### Macroscopic measurement for hair growth

To assess the hair growth process, photos of the hair-shaved areas were continuously obtained every two days from D0 to D16 using a Canon 70D digital camera (Canon Inc., Japan). The change of skin color from pink to grey indicated the transition of hair follicles from the telogen phase into the anagen phase [34]. Therefore, the date of first observing the skin turning grey was recorded, and the percentage of anagen entry rate (%) for each group was calculated as follows:

$$\text{Anagen entry rate (\%)} = \frac{\text{Number of mice with grey skin}}{12} \times 100\%.$$

In addition, the hair coverage percentage of each group was calculated by Image J and represented as follows:

$$\text{Hair coverage percentage (\%)} = \frac{\text{Sum of the area covered by regrowth hair (cm}^2\text{)}}{4 \times 1.5 \text{ (cm}^2\text{)} (\text{Initial shaving area})} \times 100\%.$$

### Histological evaluation

The collected skin samples were fixed in 4% paraformaldehyde for 24 h and embedded in paraffin. To access the number change of hair follicles, 5  $\mu\text{m}$ -thick cross-sections of the samples were prepared and stained with hematoxylin–eosin (HE). To access angiogenesis and hair follicles proliferation, sliced paraffin sections were immunohistochemically stained with anti-CD31 (1:500 dilutions, ab182981, Abcam, Cambridge, UK) and anti-Ki67 (1:500 dilutions, ab16667, Abcam) respectively overnight at 4 °C. Then incubated with horseradish peroxidase-conjugated polymer anti-rabbit antibody (Dako, Denmark) for 1 h. The number of CD31-positive blood vessels and the percentage of Ki67-positive proliferating hair follicles cells were counted using an optical microscope (Nikon Corp., Japan) and obtained with the digital camera (Nikon DS-Ri2, Japan) and NIS-Elements AR 3.2 software. Images were 600  $\times$  600 pixels with no downstream image processing and then analyzed with *Image J* (NIH

*Image J* system, USA). At least three random fields were selected for each sample.

### Western blot analysis for tissues

To evaluate the expression of AR in vivo, approximately 2000 hair follicles were separated from the collected skin samples under Stereoscope (Olympus, Japan). Hair bulbs were then preserved and ground to powder in liquid nitrogen. Subsequently, the powder was incubated in clod RIPA buffer (Servicebio, China) and centrifuged at 16,000 rpm for 20 min at 4 °C to obtain total amount protein. Other steps were the same as a general western blot procedure for cell lysate. The primary antibodies used were Anti-AR (1:1000 dilution, AF6137, Affinity Biosciences, USA) and anti- $\beta$ -actin (1:2000 dilution, ab8226, Abcam, USA).

### Cell culture and experimental design

Human dermal papilla cells (hDPCs) were purchased from ScienCell (California, USA) and cultured in Dulbecco's Modified Eagles Medium-Nutrient Mixture F-12 (DMEM/F-12, Gibco, USA) containing 10% Fetal bovine serum (FBS, HyClone, USA) and 1% penicillin–streptomycin antibiotic (Gibco, USA) at 37 °C in a 5% CO<sub>2</sub> environment. Media were changed every 5 days, and cells were used up to passages 4 for subsequent experiments.

In the following vitro study, we separate the experimental groups in 3 and each group contains 4 subgroups to evaluate the effect of CEFFE and DHT on hDPCs:

Group<sup>CEFFE</sup> (only treated with CEFFE), Group<sup>DHT</sup> (only treated with DHT (Solarbio, China)), Group<sup>DHT+CEFFE</sup> (treated with CEFFE and DHT). The specific grouping method was shown in Table 1. Cells were observed and photographed by inverted phase-contrast microscopy (Nikon Eclipse TS100) with Nikon DXM1200 camera (Nikon, Japan) and NIS-Elements AR 3.2 software with 1290  $\times$  1024 pixels without downstream image processing.

### Cell proliferation assay

Cell proliferation was evaluated by CCK-8 assay (Beyotime, China). hDPCs were seeded in 96-well plates ( $6 \times 10^3$  cells per well) with a standard medium for 24 h and then treated with a fresh medium containing corresponding drug concentrations for another 72 h. Then the medium was replaced and incubated with CCK-8 reagents diluted in DMEM (1:9) for 2 h at 37 °C. The optical density value of each well was detected at a wavelength of

**Table 1** In Group<sup>CEFFE</sup>, hDPCs were incubated with different concentrations of CEFFE (0, 50, 250, 500 µg/mL; 0 µg/mL CEFFE as control)

Groups	Name	Treatments
Group <sup>CEFFE</sup>	Group <sup>CEFFE_0</sup>	0 µg/mL CEFFE (Control)
	Group <sup>CEFFE_50</sup>	50 µg/mL CEFFE
	Group <sup>CEFFE_250</sup>	250 µg/mL CEFFE
	Group <sup>CEFFE_500</sup>	500 µg/mL CEFFE
Group <sup>DHT</sup>	Group <sup>DHT_0</sup>	0 µM DHT (Control)
	Group <sup>DHT_1</sup>	1 µM DHT
	Group <sup>DHT_10</sup>	10 µM DHT
	Group <sup>DHT_100</sup>	100 µM DHT
Group <sup>DHT+CEFFE</sup>	Group <sup>DHT_100+CEFFE_0</sup>	100 µM DHT + 0 µg/mL CEFFE (Control)
	Group <sup>DHT_100+CEFFE_50</sup>	100 µM DHT + 50 µg/mL CEFFE
	Group <sup>DHT_100+CEFFE_250</sup>	100 µM DHT + 250 µg/mL CEFFE
	Group <sup>DHT_100+CEFFE_500</sup>	100 µM DHT + 500 µg/mL CEFFE

In Group<sup>DHT</sup>, hDPCs were incubated with different concentrations of DHT (0, 1, 10, 100 µM; 0 µM DHT as control). In Group<sup>DHT+CEFFE</sup>, hDPCs were incubated with 100 µM DHT and different concentrations of CEFFE (0 + 100, 50 + 100, 250 + 100, 500 µg/mL + 100 µM; 0 µg/mL CEFFE + 100 µM DHT as control)

450 nm by a microplate reader (SpectraMAX190, Molecular Technologies, Japan).

#### Cell cycle and apoptosis assays

Flow cytometry (Beckman Coulter, USA) was used for cell cycle and apoptosis assays. hDPCs were cultured in 6-well plates ( $2 \times 10^5$  cells per well) for 24 h and treated as described above for either 48 h for cell cycle assay or 96 h for apoptosis assay. Then cells were harvested and washed with PBS 3 times. Cell cycle analysis kit (Beyotime, China) was used for cell cycle analysis, and Annexin V-FITV/PI apoptosis analysis kit (BD Biosciences, USA) was used for apoptosis assays following the manufacturer's protocol. Results were analyzed by Kaluza Analysis Software v.2.0.

#### Enzyme-linked immunosorbent assay

hDPCs were cultured in 6-well plates at a density of  $4 \times 10^5$  cells for 24 h, and the culture medium was changed as described above for another 72 h. After being lysed with RIPA (Servicebio, China), the lysis supernatant from different samples was collected and analyzed using

a DHT Quantizing ELISA kit (DB52021, IBL, German) following the manufacturer's protocol.

#### Real-time quantitative-PCR (RT-qPCR)

hDPCs were seeded in 6-well plates ( $4 \times 10^5$  cells per well) for 24 h and treated with corresponding drugs for 72 h. All cellular RNA was then extracted using Total RNA Extraction Reagent (EZBioscience, USA). 1 µg of the extracted RNA was reversed to cDNA using a reverse transcription master mix (EZBioscience, USA). Then RT-qPCR was conducted using an SYBR green qPCR master mix (ROX2 plus, EZBioscience, USA). The cycling parameters were 95 °C for 5 min, then 40 cycles at 95 °C for 10 s, followed by 60 °C for 30 s. At least three technical replicates were performed for each sample. Relative expression levels were calculated using the  $2^{-\Delta\Delta CT}$  method and were presented as fold-change compared to GAPDH expression. The primers for RT-qPCR are listed in Table 2.

#### Western blot analysis for cell

hDPCs were seeded in 10 cm plates at a density of  $6 \times 10^5$  cells for 24 h and then treated with various mediums for

**Table 2** Primer pairs used in RT-qPCR

Gene names	Forward: 5'–3'	Reverse: 3'–5'
AR	CTCTCTCAAGATTTGGATGGCT	CACTTGCACAGAGATGATCTCTGC
SRD5A2	TTTCTCGGTGAGATCATTGAATG	TTAGGTAGAACCATATGGTGGTG
AKR1C2	CCTATGCACCTCCAGAGTTTC	TTCGGATGGCCAGTCCAAC
AKR1C4	TCATGGAGAAGTGTAGGATGCAG	TCATGGAGAAGTGTAAAGGATGCA
GAPDH	GGGAAGCTTGTCATCAATGAA	AGAGATGACCCCTTTTGCTC

72 h. Next, total proteins from different samples were obtained and quantified using a BCA assay. Equal amount of proteins was loaded and separated using 10% sodium dodecyl sulfate–polyacrylamide gel and transferred to polyvinylidene fluoride membranes. The membranes were then incubated with the primary and secondary antibodies (1:5000 dilution, 111-035-045, Jackson ImmunoResearch) and visualized using enhanced chemiluminescence (Pierce, USA). The primary antibodies used were Anti-AR (1:1000 dilution, AF6137, Affinity, USA), Anti-SRD5A2 (1:1000 dilution, Ab124877, Abcam, USA) and anti- $\beta$ -actin (1:2000 dilution, Ab8226, Abcam, USA).

### Statistical analysis

All Data were presented as the mean  $\pm$  standard deviation, and each value was averaged or calculated using three unbiased samples collected in the experimental data. Statistical analysis was performed using an independent-sample *t*-test or one-way analysis of variance, followed by Tukey's post hoc test on SPSS 13.0 software (SPSS, Inc., Chicago, USA). A statistically significant difference was reported if  $P < 0.05$ .

## Results

### CEFFE contains low doses of sex hormones and is not immunogenic or genotoxic

The testosterone level in CEFFE was  $0.18 \pm 0.08$  ng/mL, which was well below normal physiological levels (6.00–27.10 ng/mL), and the estradiol concentration in CEFFE was  $0.02 \pm 0.01$  ng/mL, within the normal physiological range (0.011–0.044 ng/mL) (Additional file 2: Fig. S1A). Results of the in vitro cytotoxicity test showed that cell survival rates were 2%, 56%, 87%, and 125% for 100%, 50%, 25%, and 12.5% CEFFE, respectively, with potential cytotoxicity at CEFFE volume fractions  $> 25\%$  (Additional file 2: Fig. S1B). In the intracutaneous reactivity test, no erythema and edema was observed in each animals in 24, 48, 72 h after injection of CEFFE, and the difference between the mean scores of the CEFFE experimental group and the blank control group was  $< 1$  (Additional file 1: Table S2). In the system in toxicity assay, no signs of systemic toxicity such as weight loss or death were observed in CEFFE experimental group (Additional file 1: Tables S3, S4). In the pyrogen test, the increase in body temperature in three rabbits was  $0^\circ\text{C}$ ,  $0^\circ\text{C}$  and  $0^\circ\text{C}$  respectively. The combined increase in body temperature was  $0^\circ\text{C}$ , which satisfied the criteria of  $< 0.6^\circ\text{C}$  for each rabbit or  $< 1.3^\circ\text{C}$  for the total increase in body temperature. CEFFE was judged to have no pyrogenic effect. The above experiments were combined to determine that CEFFE was non-immunogenic. In Ames assay, the negative control and the positive control met the criteria. CEFFE did not increase the number of colonies of 4

strains by twofold or more compared with the negative control (Additional file 1: Table S5). In MLA assay, the negative control and the positive control met the criteria, and the frequency of CEFFE induced mutations in the TK gene was similar to that of the negative control (Additional file 1: Table S6). The results of these two experiments showed that CEFFE was non-genotoxic.

### CEFFE reversed hair regrowth delay induced by DHT through blocking AR

During the experiment, no adverse health events were recorded. To determine whether CEFFE could promote hair regrowth in DHT-induced AGA mice models, consecutively taken photographs on shaved area was evaluated. Skin color, anagen entry rate (%) and hair coverage percentage (%) for different groups were compared and calculated as described previously. All mice were depilated and start from telogen phase to eliminate inter-subject differences and allow synchronous hair regeneration. Normally, the shaved skin of C57BL/6 mice was pink during the telogen phase and darkens as entering anagen phase. As shown in Fig. 1C, seven days after depilation, the skin of control mice was pigmented (anagen phase), whereas Model group mice was still pink until D10, indicating a significant delay in the reentry of the hair follicles into the anagen phase. However, in the CEFFE treatment groups, the skin color changed from pink to grey on D8, D6, and D8 respectively for CEFFE<sup>Low</sup>, CEFFE<sup>Middle</sup>, and CEFFE<sup>High</sup> groups, which are much earlier than the Model group (Fig. 1D). By D14, the CEFFE treatment group displayed more than 60% hair regrowth, reached more than 90% hair regrowth after D16. (Fig. 1E) The hair regrowth of the CEFFE treatment group showed statistical significance compared to the Model group with  $P < 0.05$ .

### CEFFE promoted DPCs proliferation and enhanced angiogenesis

To investigate DHT-induced histological changes, dorsal skin samples were taken from all subjects and studied through HE staining and immunohistochemistry for proliferation marker Ki67 and angiogenesis marker CD31 (Fig. 2A–C). The number of hair follicles per field was counted quantitatively, and the morphology of the inner and out root sheath of hair was displayed. There was no significant difference in HF number and morphology among groups ( $P > 0.05$ ), which might be due to a too short DHT modeling time (Fig. 2D). The immunohistochemical stain of CD31 showed that the number of blood vessels per field surrounding dermal papillae was significantly decreased in the Model group ( $6.8 \pm 2.59$ ) compared with the control group ( $11.0 \pm 2.92$ ) ( $P < 0.05$ ). The number of CD31-positive blood vessels in all CEFFE treated groups

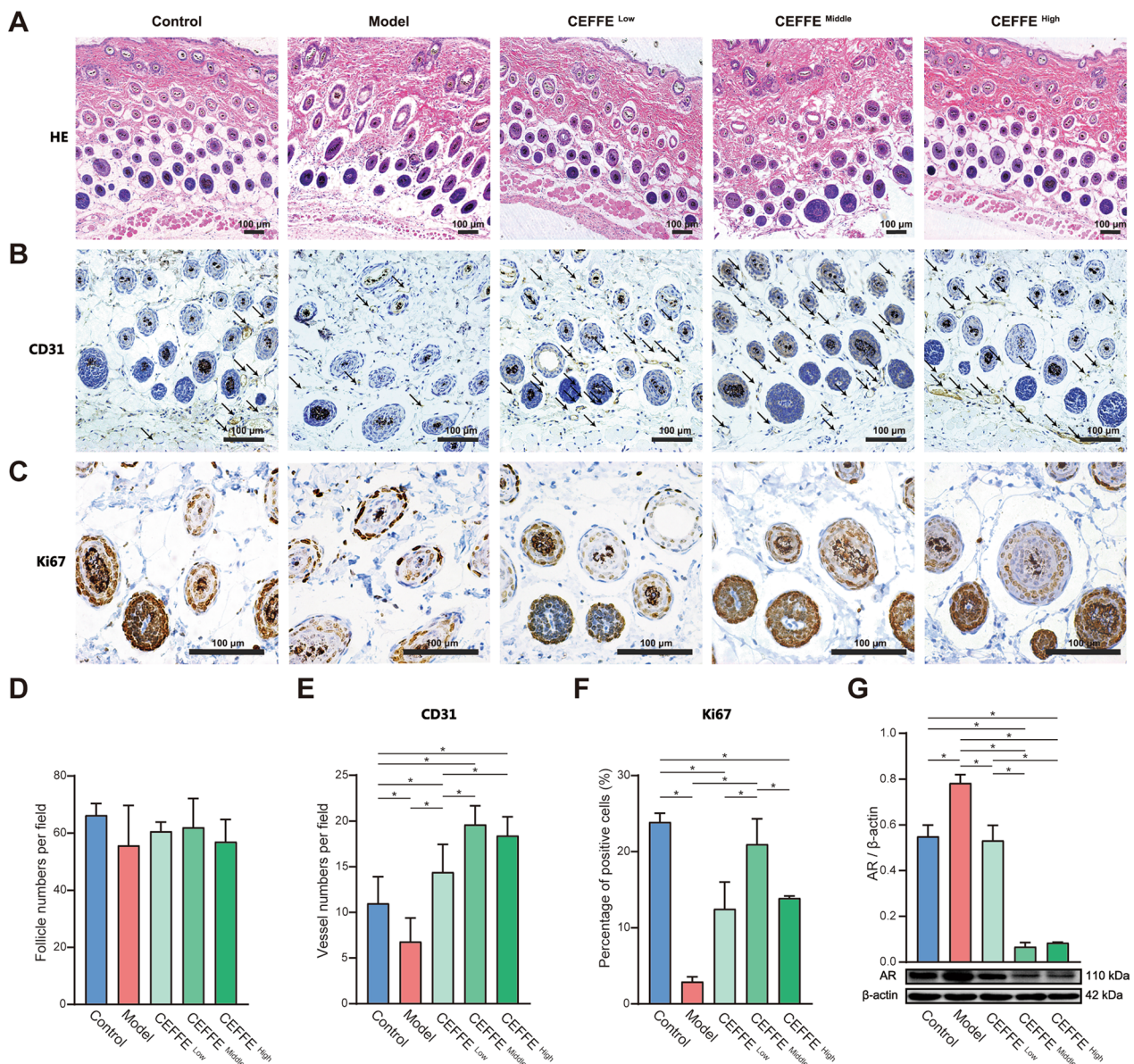


**Fig. 2** Sagittal sectional views of histological observation of hair follicles in C57BL/6 mice. **A** HE staining on dorsal skin taken from the shaved area with 4× objective lens. Scale bar = 100 μm. **B** Quantitative analysis on the number of hair follicles. **C** CD31 immuno-histochemical staining of dermal sections with 10× objective lens (black arrows indicate CD31—positive micro-vessels). Scale bar = 100 μm. **D** Quantitative analysis of CD31 staining surrounding hair follicles. **E** Ki67 immunohistochemically staining of dermal sections with 20× objective lens. Scale bar = 100 μm. **F** Quantitative analysis of Ki67 staining inside hair follicles. **G** Western blot analysis probing for androgen receptor (AR) after CEFFE treatment. Density values were presented in arbitrary units (AU). Original data was presented in Additional file 2: Fig. S3. Data represent the mean ± SD; \**P* < 0.05

(14.4 ± 3.04 for CEFFE<sup>Low</sup>; 19.61 ± 2.07 for CEFFE<sup>Middle</sup>; 18.4 ± 2.08 for CEFFE<sup>High</sup>) was much higher compared to the Model group (*P* < 0.05), with the highest in the CEFFE<sup>Middle</sup> group (Fig. 2E). The immunohistochemical stain of Ki67 showed a decrease in Ki67-positive proliferation cells for Model mice (3.38 ± 0.76%), compared to the control group 23.93 ± 0.98% (*P* < 0.05).

However, in the CEFFE treatment group, the number of Ki67-positive increased sharply after being treated with CEFFE (Fig. 2F). 16.17 ± 11.89% for CEFFE<sup>Low</sup>; 24.84 ± 20.22% for CEFFE<sup>Middle</sup>; 14.79 ± 13.86% for CEFFE<sup>High</sup> (*P* < 0.05) respectively. Among three treatment groups, CEFFE<sup>Middle</sup> showed the best proliferation promotion ability.

### CEFFE decreased the DHT-induced high expression of AR

To evaluate the regulation effect of CEFFE on AR expression in vivo, western blot probing for AR in hair bulbs was performed. Results showed that the expression of AR in the Model group was much higher than in the control group ( $P < 0.05$ ), indicating DHT upregulate AR expression. In contrast, the expression of AR was decreased in the CEFFE treatment group compared to the Model group, and CEFFE<sup>Middle</sup> group showed most robust inhibition of AR protein expression (Fig. 2G). Therefore, CEFFE<sup>Middle</sup> may be the optimal dosing regimen to cure DHT-induced AGA in this study.

### CEFFE reversed decrease in proliferation and abnormal cell cycle arrest of hDPCs caused by DHT

To investigate the influence of CEFFE on hDPCs proliferation with or without DHT, direct observation using light microscopic and CCK-8 assay were applied to different groups. In Group<sup>CEFFE</sup>, CEFFE showed a consistent ability to promote cell proliferation regardless of CEFFE concentration. The optimal proliferation of hDPCs was detected at CEFFE concentration of 50  $\mu\text{g}/\text{mL}$  (Fig. 3A). In Group<sup>DHT</sup>, fewer cells were observed following the increase in concentration of DHT treatment, indicating a stronger proliferation inhibition (Fig. 3B). Therefore, 100  $\mu\text{M}$  DHT was used as the modeling concentration to simulate the high DHT concentration in the patients with AGA. For Group<sup>DHT+CEFFE</sup>, results showed that CEFFE rescued hDPCs from DHT (100  $\mu\text{M}$ )-related stress. The 250  $\mu\text{g}/\text{mL}$  of CEFFE treatment among all different concentrations has the best therapeutic effects (Fig. 3C).

To further explore potential mechanisms of the growth-promoting effect of CEFFE on hDPCs with and without DHT, cell-cycle and apoptosis analysis were performed using flow cytometry. In Group<sup>CEFFE</sup> (Fig. 3D), CEFFE led to a reduce amount of cells in G2/M- phase and an increase amount of cells in S-phase comparing to control subgroup ( $P < 0.05$ ). On the contrary, in Group<sup>DHT</sup>, there was a significant increase ( $P < 0.05$ ) of hDPCs in G2/M phases as compared to the untreated cells, with 100  $\mu\text{M}$  DHT showed the most substantial G2/M arrest effect (Fig. 3E). In Group<sup>DHT+CEFFE</sup>, CEFFE showed the ability to reverse cell cycle arrest at the G2/M phase induced by 100  $\mu\text{M}$  DHT in a dose-dependent manner and showed the best effect at 500  $\mu\text{g}/\text{mL}$  (Fig. 3F).

### CEFFE inhibited apoptosis induced by DHT in hDPCs

In apoptosis analysis, early apoptotic cells (Annexin V-positive, PI-negative) and late apoptotic cells (Annexin V-positive, PI-positive) were evaluated (Fig. 4A). As Fig. 4B showed, the amount of apoptotic hDPCs was significantly reduced when treated with 250  $\mu\text{g}/\text{mL}$  CEFFE in Group<sup>CEFFE</sup> ( $P < 0.05$ ). In contrast, a dosage-dependent apoptotic increase was observed upon DHT treatment in Group<sup>DHT</sup> (Fig. 4C) ( $P < 0.05$ ). In Group<sup>DHT+CEFFE</sup> (Fig. 4D), CEFFE was shown to inhibit apoptosis induced by DHT by affecting DHT-induced G2/M cell cycle arrest ( $P < 0.05$ ).

### CEFFE decreased intracellular DHT concentration and reduced AR expression in hDPCs

An ELISA assay was applied to evaluate the effect of CEFFE and DHT on intracellular DHT concentration. In Group<sup>CEFFE</sup> and Group<sup>DHT</sup>, while the concentration of intracellular DHT showed a rising trend, the maximal change in Group<sup>DHT</sup> varied over five orders of magnitude, and the maximal variation in Group<sup>CEFFE</sup> was only two orders of magnitude. In Group<sup>DHT+CEFFE</sup>, the intracellular DHT concentration decreases as CEFFE increase in concentration (Fig. 5A). Meanwhile, we have test DHT production-related enzymes and metabolism-related enzymes. In the absence of DHT, 250 and 500  $\mu\text{g}/\text{mL}$  of CEFFE caused a decrease in 5 $\alpha$ -reductase type II (SRD5A2) expression in hDPCs ( $P < 0.05$ , Additional file 2: Figs. S2A, B, S5). The expression of enzymes associated with DHT metabolism (AKR1C2 and AKR1C4) were significantly increased in the presence or absence of DHT, with the most pronounced effect at 500  $\mu\text{g}/\text{mL}$  of CEFFE ( $P < 0.05$ , Additional file 2: Fig. 2C, D).

Besides ELISA, in order to evaluate the expression level of AR in hDPCs cells, RT-qPCR and Western blot were performed for further analysis. As results showed, DHT significantly increased the mRNA concentrations (Fig. 5B) and protein expressions of AR (Fig. 5C) in Group<sup>DHT</sup> compared to control. However, the AR expression was remarkably inhibited by CEFFE in a dose-dependent manner with or even without DHT treatment, suggesting CEFFE inhibit AR signaling pathway by suppressing the expression of the AR gene and corresponding AR protein synthesis. This result was consistent with vitro experimental results.

(See figure on next page.)

**Fig. 3** Effect of CEFFE (0, 50, 250, 500  $\mu\text{g}/\text{mL}$ ; 72 h), DHT (0, 1, 10, 100  $\mu\text{M}$ ; 72 h) and DHT + CEFFE (100  $\mu\text{M}$  DHT + 0, 50, 250, 500  $\mu\text{g}/\text{mL}$  CEFFE; 72 h) on Human dermal papilla cells (hDPCs) proliferation and cell cycle. **A–C** Morphology of hDPCs in Group<sup>CEFFE</sup>, Group<sup>DHT</sup> and Group<sup>DHT+CEFFE</sup> and its relevant quantitative analysis of hDPCs proliferation detected by the CCK-8 assay among different groups. **D–F** hDPCs cell cycle distribution analyzed by flow cytometry in Group<sup>CEFFE</sup>, Group<sup>DHT</sup> and Group<sup>DHT+CEFFE</sup> and their quantitative analysis of cell cycle distribution. Scale bar = 200  $\mu\text{m}$ ; Data represent the mean  $\pm$  SD;  $n = 3$ ; \* $P < 0.05$

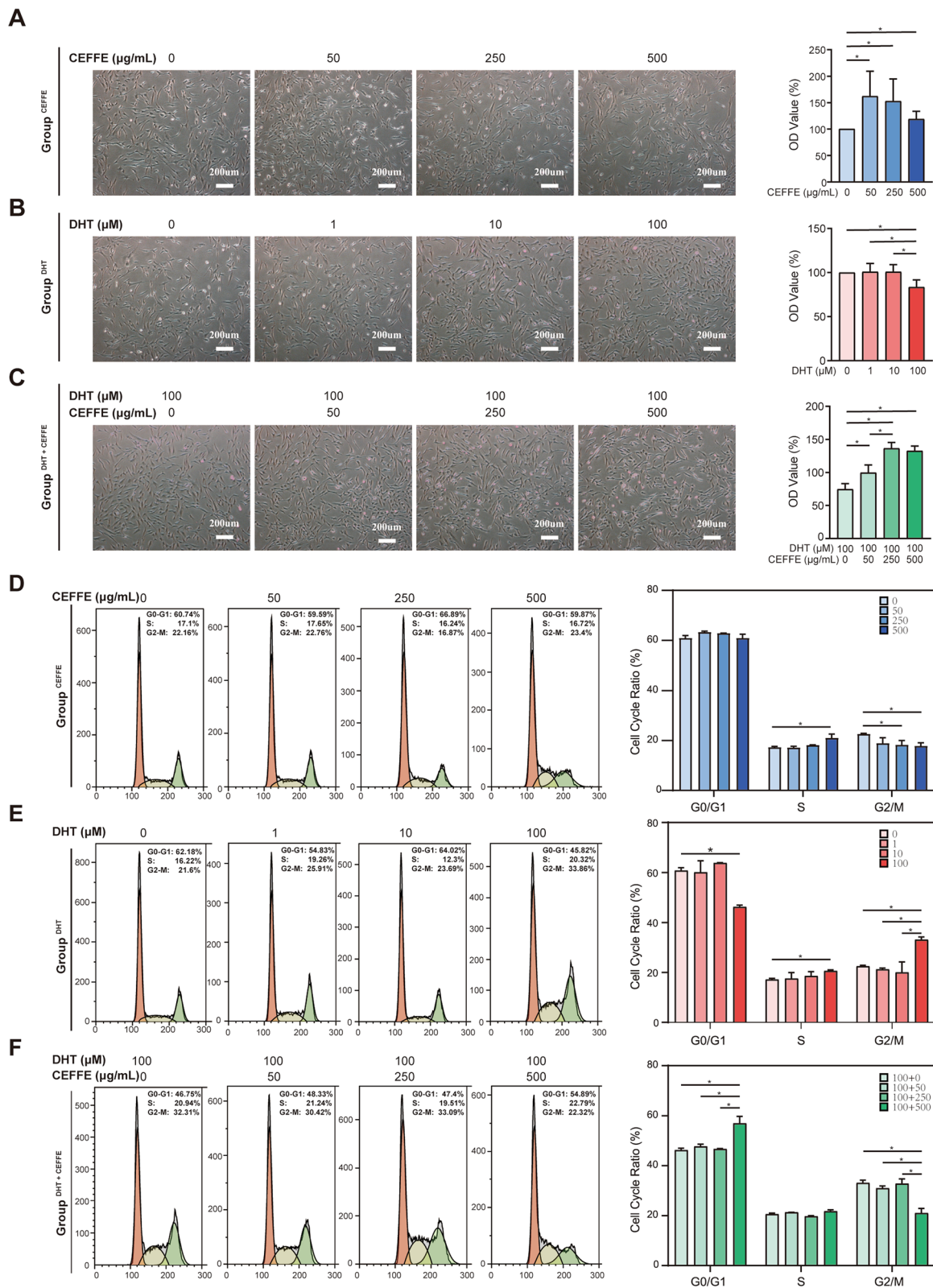


**Fig. 3** (See legend on previous page.)

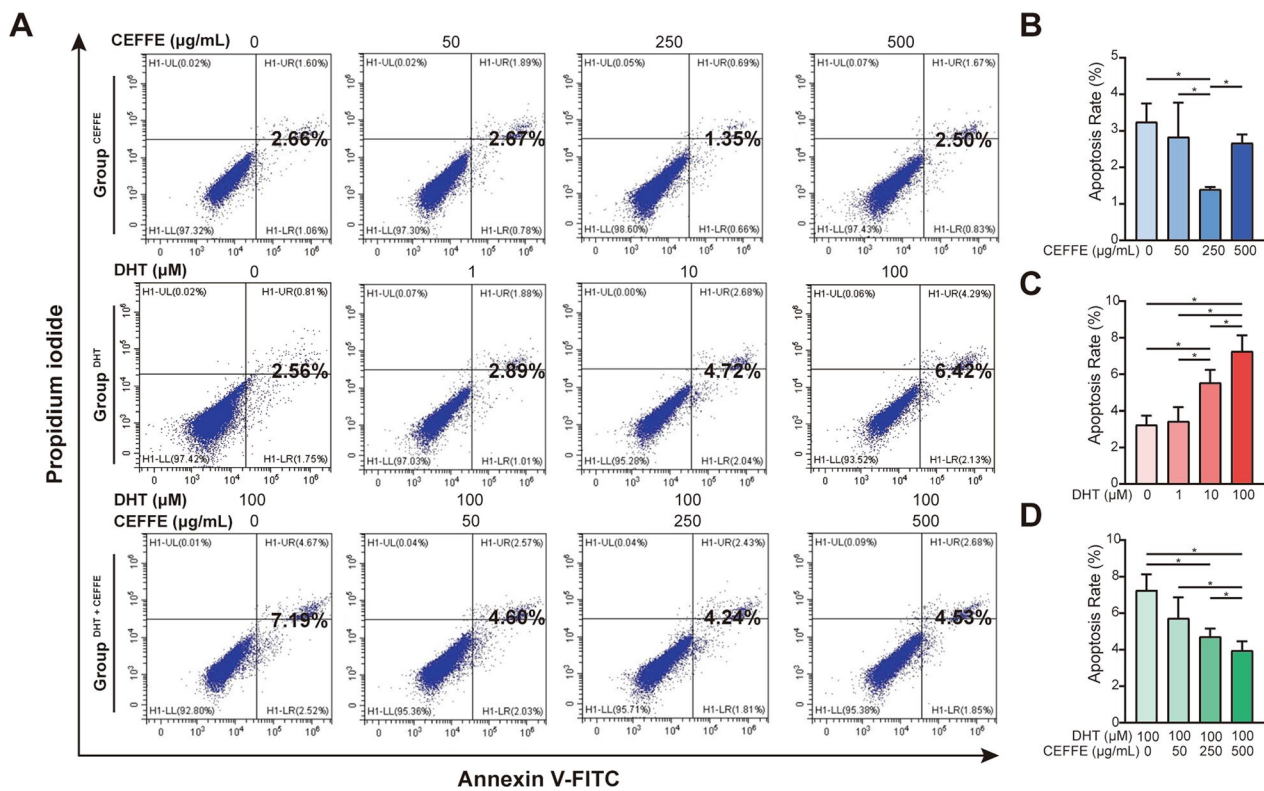


**Fig. 4** Effect of CEFFE (0, 50, 250, 500 μg/ml; 72 h), DHT (0, 1, 10, 100 μM; 72 h) and DHT + CEFFE (100 μM DHT + 0, 50, 250, 500 μg/ml CEFFE; 72 h) on cell apoptosis. **A** Effect of CEFFE, DHT and DHT + CEFFE on hDPCs apoptosis was assessed with flow cytometry with Annexin V-FITC/PI staining. **B–D** Quantitative analysis of the cell apoptosis assay among different groups. Data represent the mean ± SD;  $n = 3$ ;  $*P < 0.05$

## Discussion

AGA is the most common hair disorder and thus requires more satisfactory treatments. Recent advances in regenerative therapies, including stem cells and platelet-rich plasma, which mainly depend on bioactive factors, have raised new hopes and paved the way for new therapies against hair loss [35–38]. However, concerns about the biosafety of those biological therapies have hindered their clinical application. CEFFE, which contains similar bioactive factors to stem cells' paracrine composition, was raised as a cell-free strategy to overcome these challenges [24, 39]. In the current study, we proved the safety and therapeutic effect of CEFFE and provided multilevel biological evidence to unravel the underlying mechanism in vivo (DHT-induced mice) and in vitro (hDPCs).

Hormones should be considered when using CEFFE. We have detected testosterone, dihydrotestosterone, estradiol and progesterone levels in CEFFE from 20 female samples via ELISA test. The results showed both of the testosterone and dihydrotestosterone were undetectable and the progesterone level was barely detectable. We have also tested hormone levels in male samples, which indicated that testosterone concentration was very low and the estradiol levels with normal range. It can be

presumed that hormone levels in CEFFE have no effect on AGA treatment. Meanwhile, we have also tested the immunogenicity and genotoxicity of CEFFE, and combined results prove the safety of CEFFE due to its cell-free characteristics.

Hair follicles in AGA patients were remodeled during cyclical periods of growth (anagen), regression (catagen), and rest (telogen) [40, 41]. The length of the rapid growth stage of anagen mainly contributes to hair growth. Therefore, maintaining the anagen cycle was vital for the treatment of AGA. Our results confirmed that, in DHT-induced AGA mice models, the color change of mice skin from pink to grey was later, and the hair coverage percentage was lower than in the control group. Those phenomena indicated that DHT could short catagen phases and slow down the rate of hair growth. On the other hand, we observed that CEFFE treatment could reverse this situation, presenting as the extension of anagen phased and the acceleration hair growth rate. Moreover, we observed that CEFFE<sup>Middle</sup>-frequency might have a better therapeutic effect than other CEFFE treatment groups.

Previous studies show that DPCs in hair follicles regulates the hair cycle [42]. Specifically, in DPCs, DHT was

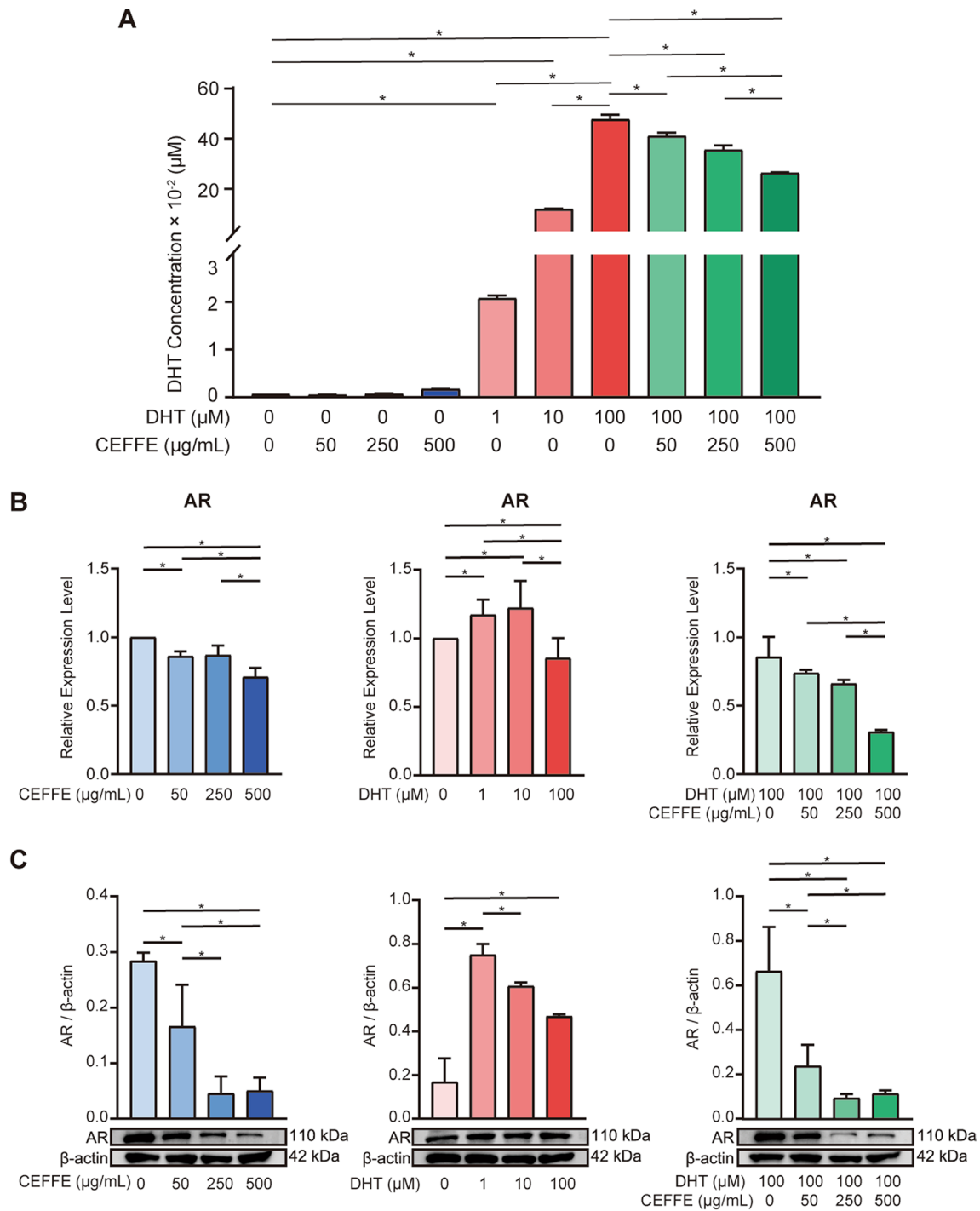


**Fig. 5** Effect of CEFFE (0, 50, 250, 500 µg/ml; 72 h), DHT (1, 10, 100 µM; 72 h) and DHT + CEFFE (100 µM DHT + 50, 250, 500 µg/ml CEFFE; 72 h) on the intracellular DHT concentration and AR expression of hDPCs. **A** Quantitative analysis of DHT concentration using ELISA. **B** RT-qPCR analysis of AR mRNA expression after culturing hDPCs with CEFFE, DHT and DHT + CEFFE, respectively. qRT-PCR analysis showed the expression of AR was increased after DHT treatment but declined after co-incubation with DHT and CEFFE. **C** Western blot for AR after treating hDPCs with CEFFE, DHT and DHT + CEFFE. Original data was presented in Additional file 2: Fig. 4. It revealed an increase in the expression of AR after incubating with DHT but decreased after co-incubation with DHT and CEFFE. Data represent the mean ± SD; n = 3; \*P < 0.05

bound to AR, and the hormone-receptor complex activates the target gene to regulate anagen-to-catagen transition [43]. Thus, the direct influence on the state of DPCs or the indirect influence on DHT/AR may influence the progression of AGA. In vivo study, although the number and the morphology of mouse hair follicles in the Model group showed no significant difference from the Control group, the quantification of Ki67-positive cells showed a significant decline. However, this trend could be reversed by CEFFE treatment, especially in the CEFFE<sup>Middle</sup> group, presenting as the protective effect of hair follicles cells. In addition, the result of the in vitro experiments was consistent with that of the in vivo experiment. In vitro study, DHT reduced the proliferation of hDPCs in a dose-dependent manner, and 100  $\mu$ M of DHT showed the most potent inhibition, the same as previously reported [44].

Moreover, we observed promotion in the proliferation of hDPCs after culturing with CEFFE regardless of the presence or absence of DHT. In other studies, HGF was associated with the span of the hair follicle stages, and platelet-derived growth factor (PDGF) promotes and maintains the anagen stage. Thus, we speculate that HGF and PDGF may play a crucial role in hair cycle control [45–47]. Furthermore, we also demonstrated that the promotion effect of CEFFE on hDPCs proliferation might be due to the inhibition of cell cycle arrest and apoptosis. In Group<sup>DHT</sup>, we found that DHT induced G2/M cell cycle arrest and increased the apoptotic rate of hDPCs. In contrast, the G2/M cell cycle arrest was abrogated, and the cell apoptosis rate decreased after culturing with CEFFE in Group<sup>CEFFE</sup> as well as Group<sup>DHT+CEFFE</sup>.

At the level of mechanism study, we considered that CEFFE could exert a therapeutic role by mediating DHT/AR pathway. In vitro study, the result of ELISA showed that intracellular concentration of DHT was significantly increased after culturing hDPCs with DHT, which was almost 20 times larger than that without DHT treatment. On the contrary, in Group<sup>DHT+CEFFE</sup>, the intracellular concentration of DHT declined in a dose-dependent manner. This phenomenon may be related to the decline of 5 $\alpha$ -reductase type II expression, which was related to DHT production. Meanwhile, the elevated expression of DHT-degrading enzymes in hDPCs may be also favorable. There was a study confirmed that Sulforaphane increases the expression of DHT-degrading enzymes to treat AGA in mice [48]. Besides, RT-qPCR and western blot proved that CEFFE could reduce the expression of AR with or without DHT, which may block the effect of AR and DHT [49]. Furthermore, in vivo study, the result of tissue western blot also confirmed that CEFFE could inhibit AR expression in DHT-induced mice, consistent with results from cell experiments. According to previous

studies, IGF-1 could play an essential role in this process either directly via the reduction of extracellular concentration of DHT or indirectly via the inhibition of AR expression [50].

Another issue of hair loss was the insufficiency of blood supplements. Hair loss symptoms were relieved when promoting angiogenesis, such as injecting platelet-rich plasma or low-level laser therapy [51–53]. As our CD-31 immunohistochemically staining showed, DHT reduced vessels number of mice in the model group compared with the standard group. On the contrary, after treating with CEFFE, the number of CD-31 positive angiogenesis per field was significantly increased, which suggested that CEFFE could stimulate neovascularization in the presence of DHT. Increasing angiogenesis enhanced blood supply for the skin and scalp and accelerated the metabolism of DHT to reduce its impact. According to other studies, VEGF may promote angiogenesis in mice [45].

Taken together, CEFFE showed a therapeutic effect on AGA in both in vivo and in vitro models. The specific mechanism is still unclear, but it is likely due to a combination of the protection of DPCs, the regulation of DHT/AR, and the promotion of neovascularization [54]. There are certain promising prospects of CEFFE, but its application in clinical needs further in-depth study. First of all, although some factors in CEFFE were well-documented to be correlated with hair regrowth, the specific component of CEFFE still stayed unclear. There were also some factors harmful for the treatment of hair loss, which have been observed in the cell culture study that higher concentration of CEFFE did not show better results (Fig. 3A). Therefore, the specific active ingredients and the optimal treatment dose of CEFFE in clinical treatment remains to be determined.

In addition, the preparation of CEFFE was rapid, simple, convenient and straightforward with its advantage of not using any exogenous agents, and only once preparation could meet clinical needs. Excess CEFFE could be stored conveniently at -80 °C for future long-term AGA treatment. The clinical application of CEFFE is similar to ADSCs-conditioned media (ADSC-CM), which is also a cell-free liquid. Subcutaneous injection or application with micro-needling weekly of ADSC-CM for 12 weeks was demonstrated as optimal method in treating AGA, which was also an option for CEFFE [39].

As for the quality control of CEFFE from different donors, donor's age, sex, and chronic disease would impact the composition of growth factors in CEFFE, especially the chronic diseases [55, 56]. CEFFE from elder people and male have not been analyzed before. In our previous study, the concentrations of major growth factors in CEFFE from healthy young females with different age (22 to 35) and different aspiration site were

relatively stable [24]. Thus, we believe that allogenic CEFFE would be an ideal source for those patients. What's more, a combination of CEFFE with existing drugs, such as Minoxidil and Finasteride, might work better. Comparing the efficacy of CEFFE, commercially available drug, and the combination of them in treating AGA is worth to be tested in the animal studies as well as in the future clinical trials.

Therefore, CEFFE appears a potential therapeutic option for AGA treatment due to its various bioactive factors composition, the absence of immunogenic

properties, the simplicity of acquisition, and the simplicity of separation.

**Conclusion**

This study demonstrated that CEFFE promoted hair growth in AGA via mediating DHT/AR pathway in DPC to enhance cell proliferation, modulate the cell cycle, and increase neovascularization in the DHT-induced model (Fig. 6). Furthermore, anti-inflammation might be another potential mechanism for treating AGA. cell-free feature of CEFFE makes it safe to use

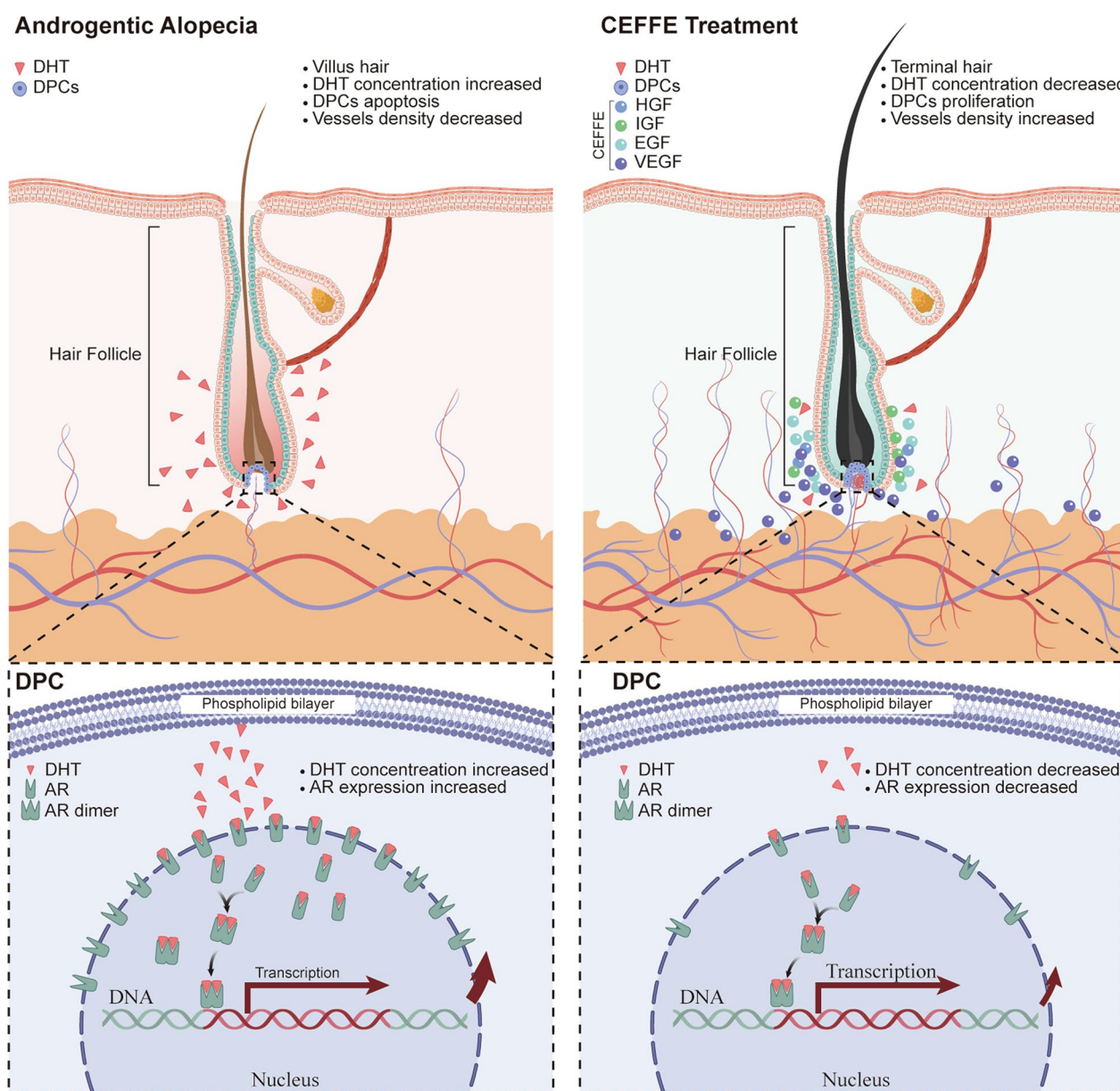


**Fig. 6** CEFFE promote hair growth in AGA via mediating DHT/AR pathway in DPC to enhance cell proliferation, modulate the cell cycle, and increase neovascularization in the DHT-induced model

without the risk of immunogenicity and genotoxicity. Thus, CEFFE could potentially be a novel and effective therapeutic strategy for AGA.

#### Abbreviations

AGA	Androgenetic alopecia
ADSCs	Adipose-derived stem cells
ANOVA	Analysis of variance
AR	Androgen receptor
CEFFE	Cell-free fat extract
CM	Conditioned media
DHT	Dihydrotestosterone
DPCs	Dermal papilla cells
ELISA	Enzyme-linked immunosorbent assay
hDPCs	Human dermal papilla cells
HE	Hematoxylin–eosin
HGF	Hepatocyte growth factor
IGF	Insulin-like growth factor
MLA assay	Mouse lymphoma TK assay
PDGF	Platelet-derived growth factor
PG	Prostaglandin
PRP	Platelet-rich plasma
RT-qPCR	Reverse transcription-quantitative polymerase chain reaction
VEGF	Vascular endothelial growth factor

#### Supplementary Information

The online version contains supplementary material available at <https://doi.org/10.1186/s13287-023-03398-1>.

**Additional file 1: Table S1.** Patient information. **Table S2.** Results of the intracutaneous reactivity test. **Table S3.** Clinical signs/observations to systemic toxicity assay. **Table S4.** Variation in the weight of the animal in systemic toxicity assay. **Table S5.** Results of Ames test. **Table S6.** Results of MLA assay.

**Additional file 2: Figure S1.** Hormone levels evaluation and in vitro cytotoxicity test results. **Figure S2.** RT-qPCR or/and western blot analysis of DHT-producing enzymes SRD5A2 and DHT-degrading enzymes in hDPCs co-cultured with CEFFE 72 h. **Figure S3.** Original data of AR western blot results in hair follicles of C57BL/6 mice. **Figure S4.** Original data of AR western blot results in hDPCs. **Figure S5.** Original data of SRD5A2 western blot results in hDPCs.

#### Acknowledgements

We would like to thank all the Shanghai Key Laboratory of Tissue Engineering members for their advice and help with this study.

#### Author contributions

The study was designed by WL1, WL2 and WZ. YC contributed to experimentation, data collection, manuscript writing and editing. ZJ contributed to data analyses, manuscript writing, editing and data visualization. YZ contributed to manuscript writing and editing. BK and CC carried out some of experiments. All authors read and approved the final manuscript.

#### Funding

This study was supported by the Shanghai Collaborative Innovation Program on Regenerative Medicine and Stem Cell Research (2019CXJQ01). The funder had no role in data collection, management, analysis, publication decision, or manuscript preparation.

#### Availability of data and materials

The datasets during the current study are available from the corresponding author on reasonable request.

#### Declarations

##### Ethics approval and consent to participate

This study adheres to the Declaration of Helsinki. This study was approved by the Ethics Committee of Shanghai Ninth People's Hospital, Shanghai Jiaotong University School of Medicine, Shanghai, China (study title: basic research of Nanofat; approval number: SH9H-2018-T22-1; date of approval: 2018.09.03) and written informed consent was obtained from all participating patients. Animal experiments were approved by the Ethics Committee of Shanghai Ninth People's Hospital, Shanghai Jiaotong University School of Medicine, Shanghai, China (study title: study on the mechanism of cell-free fat extract in the treatment of androgenic alopecia; approval number: SH9H-2021-A183-SB; date of approval: 2021.02.02).

##### Consent for publication

Not applicable.

##### Competing interests

The author declares that they have no competing interests.

##### Author details

<sup>1</sup>Department of Plastic and Reconstructive Surgery, Shanghai 9th People's Hospital, Shanghai Jiao Tong University School of Medicine, Shanghai Key Laboratory of Tissue Engineering, National Tissue Engineering Center of China, 639 ZhiZaoJu Road, Shanghai 200011, China. <sup>2</sup>Department of Biological and Environmental Engineering, Cornell University, Ithaca, USA.

Received: 11 April 2022 Accepted: 12 June 2023

Published online: 23 August 2023

#### References

- Tosti A, Piraccini BM. Androgenetic alopecia. *Int J Dermatol*. 1999;38(Suppl 1):1–7.
- Otberg N, Finner AM, Shapiro J. Androgenetic alopecia. *Endocrinol Metab Clin North Am*. 2007;36(2):379–98.
- Severi G, Sinclair R, Hopper J, English D, McCredie M, Boyle P, et al. Androgenetic alopecia in men aged 40–69 years: prevalence and risk factors. *Br J Dermatol*. 2003;149(6):1207–13.
- Xu F, Sheng Y, Mu Z, Lou W, Zhou J, Ren Y, et al. prevalence and types of androgenetic alopecia in Shanghai, China: a community-based study. *Br J Dermatol*. 2009;160(3):629–32.
- Hibberts NA, Howell AE, Randall VA. Balding hair follicle dermal papilla cells contain higher levels of androgen receptors than those from non-balding scalp. *J Endocrinol*. 1998;156(1):59–65.
- Ellis JA, Sinclair R, Harrap SB. Androgenetic alopecia: pathogenesis and potential for therapy. *Expert Rev Mol Med*. 2002;4(22):1–11.
- Ceruti JM, Leirós GJ, Balañá ME. Androgens and androgen receptor action in skin and hair follicles. *Mol Cell Endocrinol*. 2018;465:122–33.
- Stefanato CM. Histopathology of alopecia: a clinicopathological approach to diagnosis. *Histopathology*. 2010;56(1):24–38.
- Kelly Y, Blanco A, Tosti A. Androgenetic alopecia: an update of treatment options. *Drugs*. 2016;76(14):1349–64.
- Kang MJ, Choi JY, Sim WY, Lew BL. 5 $\alpha$ -Reductase inhibitors in men aged 50 years or older with androgenetic alopecia: a retrospective study. *J Am Acad Dermatol*. 2021;84(1):172–3.
- Irwig MS. Persistent sexual side effects of Finasteride: Could they be permanent? *J Sex Med*. 2012;9(11):2927–32.
- Olsen EA, Dunlap FE, Funicella T, et al. A randomized clinical trial of 5% topical minoxidil versus 2% topical minoxidil and placebo in the treatment of androgenetic alopecia in men. *J Am Acad Dermatol*. 2002;47(3):377–85.
- Rossi A, Cantisani C, Melis L, Iorio A, Scali E, Calvieri S. Minoxidil use in dermatology, side effects and recent patents. *Recent Pat Inflamm Allergy Drug Discov*. 2012;6(2):130–6.
- Chiang YZ, Tosti A, Chaudhry IH, et al. Lichen planopilaris following hair transplantation and face-lift surgery. *Br J Dermatol*. 2012;166(3):666–370.

15. Won CH, Yoo HG, Kwon OS, et al. Hair growth promoting effects of adipose tissue-derived stem cells. *J Dermatol Sci*. 2010;57(2):134–7.
16. Park BS, Kim WS, Choi JS, et al. Hair growth stimulated by conditioned medium of adipose-derived stem cells is enhanced by hypoxia: evidence of increased growth factor secretion. *Biomed Res*. 2010;31(1):27–34.
17. Shin H, Ryu HH, Kwon O, Park BS, Jo SJ. Clinical use of conditioned media of adipose tissue-derived stem cells in female pattern hair loss: a retrospective case series study. *Int J Dermatol*. 2015;54(6):730–5.
18. Gimble JM, Bunnell BA, Guilak F. Human adipose-derived cells: an update on the transition to clinical translation. *Regen Med*. 2012;7(2):225–35.
19. Rosca AM, Rayia DM, Tutuianu R. Emerging role of stem cells—derived exosomes as valuable tools for cardiovascular therapy. *Curr Stem Cell Res Ther*. 2017;12(2):134–8.
20. Kozłowska U, Blume-Peytavi U, Kodelja V, et al. expression of vascular endothelial growth factor (VEGF) in various compartments of the human hair follicle. *Arch Dermatol Res*. 1998;290(12):661–8.
21. Yano K, Brown LF, Detmar M. Control of hair growth and follicle size by VEGF-mediated angiogenesis. *J Clin Invest*. 2001;107(4):409–17.
22. Su HY, Hickford JG, Bickerstaffe R, Palmer BR. Insulin-like growth factor 1 and hair growth. *Dermatol Online J*. 1999;5(2):1.
23. Angunsi N, Taura A, Nakagawa T, et al. Insulin-like growth factor 1 protects vestibular hair cells from aminoglycosides. *NeuroReport*. 2011;22(1):38–43.
24. Yu Z, Cai Y, Deng M, et al. Fat extract promotes angiogenesis in a murine model of limb ischemia: a novel cell-free therapeutic strategy. *Stem Cell Res Ther*. 2018;9(1):294.
25. Li T, Sui Z, Matsuno A, et al. Fabrication and evaluation of a xenogeneic decellularized nerve-derived material: preclinical studies of a new strategy for nerve repair. *Neurotherapeutics*. 2020;17(1):356–70.
26. Wang J, Sawyer JR, Chen L, et al. The mouse lymphoma assay detects recombination, deletion, and aneuploidy. *Toxicol Sci*. 2009;109(1):96–105.
27. Cai Y, Yu Z, Yu Q, et al. Fat extract improves random pattern skin flap survival in a rat model. *Aesthet Surg J*. 2019;39(12):NP504–14.
28. Wang X, Deng M, Yu Z, et al. Cell-free fat extract accelerates diabetic wound healing in db/db mice. *Am J Transl Res*. 2020;12(8):4216–27.
29. Yin M, Wang X, Yu Z, et al.  $\gamma$ -PGA hydrogel loaded with cell-free fat extract promotes the healing of diabetic wounds. *J Mater Chem B*. 2020;8(36):8395–404.
30. Matias JR, Malloy V, Orentreich N. Animal models of androgen-dependent disorders of the pilosebaceous apparatus. 1. The androchronogenetic alopecia (AGA) mouse as a model for male-pattern baldness. *Arch Dermatol Res*. 1989;281(4):247–53.
31. Crabtree JS, Kilbourne EJ, Peano BJ, et al. A mouse model of androgenetic alopecia. *Endocrinology*. 2010;151(5):2373–80.
32. Müller-Röver S, Handjiski B, van der Veen C, et al. A comprehensive guide for the accurate classification of murine hair follicles in distinct hair cycle stages. *J Invest Dermatol*. 2001;117(1):3–15.
33. Plikus MV. New activators and inhibitors in the hair cycle clock: targeting stem cells' state of competence. *J Invest Dermatol*. 2012;132(5):1321–4.
34. Wu YF, Wang SH, Wu PS, et al. Enhancing hair follicle regeneration by nonablative fractional laser: assessment of irradiation parameters and tissue response. *Lasers Surg Med*. 2015;47(4):331–41.
35. Uebel CO, da Silva JB, Cantarelli D, Martins P. The role of platelet plasma growth factors in male pattern baldness surgery. *Plast Reconstr Surg*. 2006;118(6):1458–66.
36. Gkini MA, Kouskoukis AE, Tripsianis G, Rigopoulos D, Kouskoukis K. Study of platelet-rich plasma injections in the treatment of androgenetic alopecia through an one-year period. *J Cutan Aesthet Surg*. 2014;7(4):213–9.
37. Cervelli V, Garcovich S, Bielli A, et al. The effect of autologous activated platelet rich plasma (AA-PRP) injection on pattern hair loss: clinical and histomorphometric evaluation. *Biomed Res Int*. 2014;2014:760709.
38. Gentile P, Garcovich S, Bielli A, Scioli MG, Orlandi A, Cervelli V. The effect of platelet-rich plasma in hair regrowth: a randomized placebo-controlled trial. *Stem Cells Transl Med*. 2015;4(11):1317–23.
39. Lee YI, Kim J, Kim J, Park S, Lee JH. The effect of conditioned media from human adipocyte-derived mesenchymal stem cells on androgenetic alopecia after nonablative fractional laser treatment. *Dermatol Surg*. 2020;46(12):1698–704.
40. Stenn KS, Paus R. Controls of hair follicle cycling. *Physiol Rev*. 2001;81(1):449–94.
41. Alonso L, Fuchs E. The hair cycle. *J Cell Sci*. 2006;119(Pt 3):391–3.
42. Yang CC, Cotsarelis G. Review of hair follicle dermal cells. *J Dermatol Sci*. 2010;57(1):2–11.
43. Ellis JA, Stebbing M, Harrap SB. Genetic analysis of male pattern baldness and the 5 $\alpha$ -reductase genes. *J Invest Dermatol*. 1998;110(6):849–53.
44. Lee MJ, Cha HJ, Lim KM, et al. analysis of the microRNA expression profile of normal human dermal papilla cells treated with 5 $\alpha$ -dihydrotestosterone. *Mol Med Rep*. 2015;12(1):1205–12.
45. Gnanan LA, Castro RF, Azzalis LA, et al. Hematological and hepatic effects of vascular epidermal growth factor (VEGF) used to stimulate hair growth in an animal model. *BMC Dermatol*. 2013;13:15.
46. Rastegar H, Ahmadi Ashtiani H, Aghaei M, Ehsani A, Barikbin B. Combination of herbal extracts and platelet-rich plasma induced dermal papilla cell proliferation: involvement of ERK and Akt pathways. *J Cosmet Dermatol*. 2013;12(2):116–22.
47. Stevens HP, Donners S, de Bruijn J. Introducing platelet-rich stroma: platelet-rich plasma (PRP) and stromal vascular fraction (SVF) combined for the treatment of androgenetic alopecia. *Aesthet Surg J*. 2018;38(8):811–22.
48. Sasaki M, Shinozaki S, Shimokado K. Sulforaphane promotes murine hair growth by accelerating the degradation of dihydrotestosterone. *Biochem Biophys Res Commun*. 2016;472(1):250–4.
49. Kang JI, Kim SC, Kim MK, et al. Effects of dihydrotestosterone on rat dermal papilla cells in vitro. *Eur J Pharmacol*. 2015;757:74–83.
50. Zhao J, Harada N, Okajima K. Dihydrotestosterone inhibits hair growth in mice by inhibiting insulin-like growth factor-1 production in dermal papillae. *Growth Horm IGF Res*. 2011;21(5):260–7.
51. Avram MR, Leonard RT Jr, Epstein ES, Williams JL, Bauman AJ. The current role of laser/light sources in the treatment of male and female pattern hair loss. *J Cosmet Laser Ther*. 2007;9(1):27–8.
52. Desai S, Mahmoud BH, Bhatia AC, Hamzavi IH. Paradoxical hypertrichosis after laser therapy: a review. *Dermatol Surg*. 2010;36(3):291–8.
53. Gupta V, Parihar AS, Sharma VK, Jain S, Singh V, Khanna N. Evaluation of platelet-rich plasma on hair regrowth and lesional T-cell cytokine expression in alopecia areata: a randomized observer-blinded, placebo-controlled, split-head pilot study. *J Am Acad Dermatol*. 2021;84(5):1321–8.
54. Kim JH, Na J, Bak DH, et al. Development of finasteride polymer microspheres for systemic application in androgenic alopecia. *Int J Mol Med*. 2019;43(6):2409–19.
55. Jia Z, Kang B, Cai Y, et al. Cell-free fat extract attenuates osteoarthritis via chondrocytes regeneration and macrophages immunomodulation. *Stem Cell Res Ther*. 2022;13(1):133.
56. Kang B, Cai Y, Jia Z, Chen C, Deng M, Zhang W, Li W. Cell-free fat extract prevents vaginal atrophy in an ovariectomized model by promoting proliferation of vaginal keratinocytes and neovascularization. *Aesthet Surg J*. 2022;42(1):55–68.

## Publisher's Note

Springer Nature remains neutral with regard to jurisdictional claims in published maps and institutional affiliations.

Ready to submit your research? Choose BMC and benefit from:

- fast, convenient online submission
- thorough peer review by experienced researchers in your field
- rapid publication on acceptance
- support for research data, including large and complex data types
- gold Open Access which fosters wider collaboration and increased citations
- maximum visibility for your research: over 100M website views per year

At BMC, research is always in progress.

Learn more [biomedcentral.com/submissions](https://biomedcentral.com/submissions)

